Chapter 3
Dynamical Analysis of Cournot Oligopoly Models: Neimark-Sacker Bifurcation and Related Mechanisms

Anna Agliari, Nicolò Pecora and Alina Szuz

Abstract This chapter describes some properties of the nonlinear dynamics emerging from two oligopoly models in discrete time. The target of this chapter is the investigation of some local and global bifurcations which are responsible for the changes in the qualitative behaviors of the trajectories of discrete dynamical systems. Two different kinds of oligopoly models are considered: the first one deals with the presence of differentiated goods and gradient adjustment mechanism, while the second considers the demand function of the producers to be dependent on advertising expenditures and adaptive adjustment of the moves. In both models the standard local stability analysis of the Cournot-Nash equilibrium points is performed, as well as the global bifurcations of both attractors and (their) basins of attraction are investigated.

3.1 Introduction

The object of the present chapter is to describe some properties of nonlinear dynamics emerging from oligopoly models in discrete time. The target of our analysis is the investigation of some bifurcations which are responsible for the changes in the qualitative behaviors of the trajectories of the iterative process.

We consider two different kinds of oligopoly models: the first one deals with the presence of differentiated goods and gradient adjustment mechanism, while the second considers the demand function of the producers to be dependent on advertising expenditures and adaptive adjustment of the moves. In both models, we perform the

A. Agliari (✉) · N. Pecora
Department of Economics and Social Sciences, Catholic University,
Via Emilia Parmense 84, 29100 Piacenza, Italy
e-mail: anna.agliari@unicatt.it

N. Pecora
e-mail: nicolo.pecora@unicatt.it

A. Szuz
Independent Researcher, Cluj-Napoca, Romania
e-mail: alina.ghirvu@ubbcluj.ro

G.I. Bischi et al. (eds.), *Qualitative Theory of Dynamical Systems, Tools and Applications for Economic Modelling*, Springer Proceedings in Complexity,
DOI 10.1007/978-3-319-33276-5_3

local stability analysis of the Cournot-Nash equilibrium point as well as a global analysis of dynamics to study bifurcations of both attractors and basins of attraction.

Being the dynamics of such models described by maps of the family $T : X \to X$, $X \subset \mathbb{R}^2$, we will see that a particular kind of bifurcation may occur, related to a pair of complex conjugated eigenvalues which crosses the unit circle, namely the Neimark-Sacker bifurcation (NS henceforth). The NS bifurcation is associated with the existence of closed invariant curves around the bifurcating fixed point.

In the nonlinear map describing the Cournotian competition with differentiated products and gradient adjustment mechanism the steady state may be destabilized via *supercritical* NS bifurcation. Such a bifurcation gives rise to an attracting closed curve around the unstable equilibrium and, through global analysis, we shall also show that different multistability situations (i.e., coexistence of attractors) may arise.

On the other hand, the oligopoly model with advertising costs allows us to analyze the effects of the occurrence of a *subcritical* NS bifurcation in which the destabilization of the equilibrium point is due to its merging with a repelling closed curve existing when the point is still stable. The occurrence of a subcritical NS bifurcation has important implications in economic models since it can be associated with corridor stability, due to the bounded basin of attraction of the stable equilibrium (its boundary being the repelling closed curve), and to catastrophic effects, since after the bifurcation the trajectories may either jump to a different attractor far from the equilibrium or diverge. Moreover, the map describing this second oligopoly setting is piecewise smooth (PW henceforth), and we shall show that even border collision bifurcations (BCB henceforth) may cause multistability phenomena as well. We recall that BCB are typical occurrences in PW map and are related to invariant sets, such as attractors or manifolds, having a contact with the border of a region where the map changes its definition. Such a contact can cause abrupt changes either in the structure or in the stability property of the colliding invariant set. Seminal papers on such topic are by Nusse et al. [16] and Nusse and Yorke [17, 18].

3.2 Some Remarks on Neimark-Sacker Bifurcations

The aim of this section is to briefly illustrate some theoretical aspects associated with the occurrence of NS bifurcation and the appearance/disappearance of closed invariant curves, that will be the objects of the analysis developed in the following parts.

To this extent, we first recall that generally a steady state loses stability through a NS bifurcation when its Jacobian matrix has two complex eigenvalues lying on the unit circle. Two kind of NS bifurcations can be distinguished:

- *supercritical* when, immediately after the bifurcation, the unstable steady state is surrounded by an *attracting closed curve* corresponding to periodic or quasi-periodic dynamics;

- *subcritical* when, immediately before the bifurcation, the stable equilibrium is surrounded by a *repelling closed curve* which shrinks and at the bifurcation merges with the fixed point leaving a repelling focus.

A typical way of investigating the occurrence of a NS bifurcation is to start from the analysis of a two-dimensional bifurcation diagram.[1] In so doing we can detect the kind of the occurring NS bifurcation and, sometimes, to find the so-called *Chenciner* points. These points correspond to the degeneracy of the NS bifurcation, they belong to the bifurcation curve and separate cases in which either a subcritical or a supercritical bifurcation occurs. Moreover, a typical and well-known structure of the bifurcation diagram, in a two-dimensional parameter plane, is given by the so-called *Arnold's tongues* issuing from a NS bifurcation curve (on this we refer to some classical texts, e.g. [10, 15], and other works like [1, 6, 8], to cite a few). Inside any tongue at least 2 cycles exist, one stable and a saddle, and a closed invariant curve exists, made up by the unstable set of the saddle cycle that connects the periodic points of the stable cycle. These periodicity regions follow the Farey summation rule, which is also known in the literature as "adding rule" [9]. This implies that the tongues are organized so that between any two periodicity regions related to the rotation numbers, say m_1/n_1 and m_2/n_2, there exists a periodicity region related to the rotation number $(m_1 + m_2)/(n_1 + n_2)$. The rational rotation is not generic only for parameter values taken exactly on the NS bifurcation curve, while soon after the bifurcation the rational rotation becomes generic: infinitely many periodicity regions fill the parameter plane densely [9]. Generally, inside any tongue we have an attracting set formed by a saddle-node connection, that is, the unstable set of the saddle n-cycle reaches the node n-cycle thus forming a closed attracting curve. The boundaries of a m/n tongue are saddle-node bifurcation curves in the case of smooth maps and BCB curve if we are dealing with PW maps.

Let us recall that the *stable* and *unstable* sets of a saddle S^* are defined as

$$W^s(S^*) = \left\{ x : \lim_{n \to +\infty} T^n(x) = S^* \right\},$$

$$W^u(S^*) = \left\{ x : \lim_{n \to +\infty} T_{jn}^{-n}(x) = S^* \right\},$$

respectively, where T_{jn}^{-n} means a suitable sequence of inverses.

In the subcritical case, the periodicity regions exist when the fixed point is still stable, implying multistability situations, but generally immediately after their appearance no saddle-node connection exists. The repelling closed curve involved with the subcritical NS bifurcation appears at the crossing of a (global) bifurcation curve γ together with an attracting one (*Chenciner bifurcation*). The curve γ originates from a Chenciner point and enters the region in which the fixed point is stable, crossing the periodicity regions. The global bifurcations occurring at the crossing of γ are an interesting and challenging field of research.

[1] Obviously the map has to depend on at least two parameters.

In particular, in the case of smooth maps, the appearance/disappearance of closed invariant curves is associated with a saddle-connection. This particular configuration is defined as a closed invariant curve formed by the merging of a branch of the stable set of a periodic point of a saddle cycle with the unstable branch of another periodic point of the same saddle, thus forming a closed connection among the periodic points of the saddle. We shall call such a situation *homoclinic loop* that can also involve a saddle cycle of period k, being related to the forward iterate map T^k, but in this case we can also obtain a *heteroclinic loop*: indeed, the map T^k exhibits k saddles points and a branch of the stable set of a saddle may merge with a branch of another periodic point of the saddle cycle. Stated in other words, if S_i, $i = 1, \ldots, k$, are the periodic points of the saddle cycle and $\alpha_{1,1} \cup \alpha_{2,i}$ ($\omega_{1,i} \cup \omega_{2,i}$) are the unstable (stable) sets of S_i, then a heteroclinic loop is given by the merging, for example, of the unstable branch $\alpha_{1,i}$ of S_i with the stable branch $\omega_{1,j}$ of a different periodic point S_j (see Fig. 3.1). Then each periodic point of the saddle cycle is connected with another one, and an invariant closed curve is so created connecting the periodic points of the saddle cycle.

Dealing with discrete maps homoclinic and heteroclinic loops are frequently replaced by homoclinic tangles. This means that a tangency between an unstable branch $W_1^u(S^*) = \cup\alpha_{1,i}$ with a stable one $W_1^s(S) = \cup\omega_{1,i}$ occurs, followed by transverse crossings of the two sets, followed by another tangency of the same sets, but on opposite side. For major details see [1, 7, 12].

For PW maps only a few works devoted their attention to the investigation on how invariant curves appear/disappear in these peculiar contexts. Below we shall show that not only homoclinic bifurcations are involved, but also border collision bifurcations may occur at the crossing of the curve γ.

3.3 A Cournot Duopoly Model with Differentiated Products: Supercritical NS Bifurcation

In the first oligopoly model we analyze, we consider a Cournotian game with differentiated goods in which boundedly rational firms apply a gradient adjustment mechanism to update the quantity produced in each period (see [2] for a complete investigation).

The demand functions of the two players are derived from an underlying CES utility function

$$U(q_1, q_2) = q_1^\alpha + q_2^\alpha, \quad 0 < \alpha \leq 1, \tag{3.1}$$

which is maximized subject to the budget constraint

$$p_1 q_1 + p_2 q_2 = 1, \tag{3.2}$$

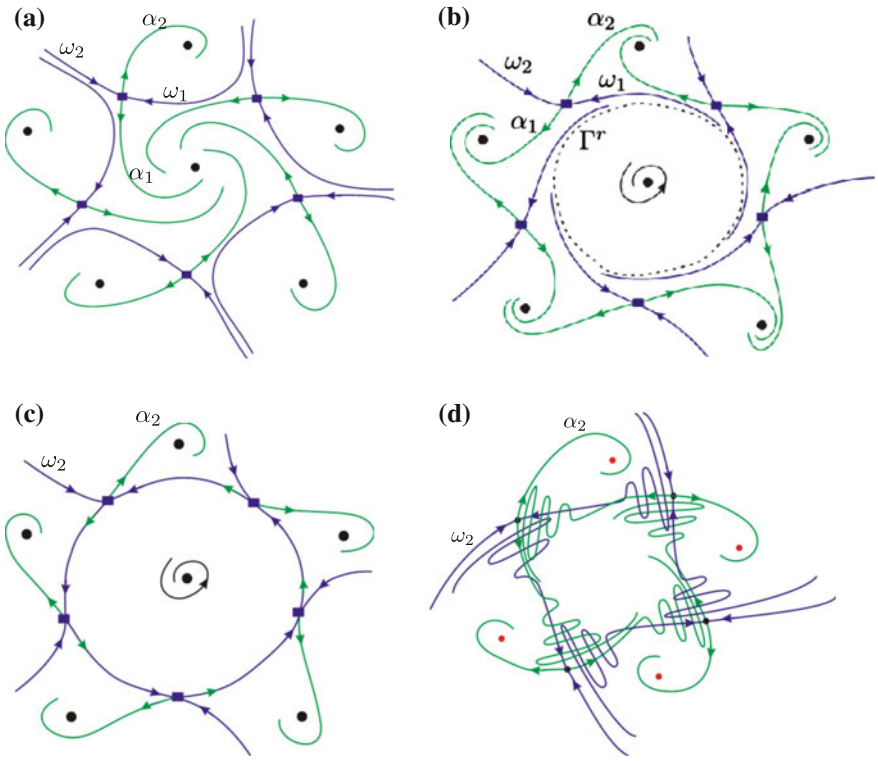

Fig. 3.1 The bifurcation mechanism associated with appearance of two closed invariant curves. **a** Stable/unstable sets before the bifurcation. **b** Two closed curves appear. **c** Heteroclinic loop. **d** Homoclinic tangle

where α gives the degree of substitutability/differentiation among the commodities, p_1 and p_2 are the prices of good 1 and 2 respectively and we assume the consumer's exogenous income equal to 1.

Maximizing (3.1) subject to (3.2) results in the inverse demand functions

$$p_1 = \frac{q_1^{\alpha-1}}{q_1^{\alpha} + q_2^{\alpha}}, \quad p_2 = \frac{q_2^{\alpha-1}}{q_1^{\alpha} + q_2^{\alpha}} \tag{3.3}$$

for goods 1 and 2 respectively.[2] From the inverse demand functions, we observe that if $\alpha = 1$ the commodities are indistinguishable and, accordingly, the consumers regard them as identical; lower values of α makes the commodities conceived as interchangeable but not quite identical. Decreasing the exponent parameter α makes

[2] We refer to [5] (Appendix A) for the mathematical computations that lead to the demand functions represented by (3.3).

the goods less close substitutes and as $\alpha \to 0$ the commodities become independent (see also [14]). Further, we assume linear cost functions given by

$$c_i\left(q_i\right) = c_i q_i, \quad i = 1, 2, \tag{3.4}$$

where c_i are constant marginal costs.

Then the profit of the i-th firm becomes

$$\Pi_i\left(q_i, q_j\right) = p_i\left(q_i, q_j\right) q_i - c_i q_i, \quad i, j = 1, 2, \quad i \neq j. \tag{3.5}$$

From the profit maximization we are able to compute the Nash equilibrium, which is unique and it is given by

$$E^* = \left(\frac{\alpha c_1^{\alpha-1} c_2^{\alpha}}{(c_1^{\alpha} + c_2^{\alpha})^2}, \frac{\alpha c_1^{\alpha} c_2^{\alpha-1}}{(c_1^{\alpha} + c_2^{\alpha})^2} \right).$$

Boundedly rational players update their quantities by an adjustment mechanism based on a local estimate of the marginal profit

$$\Phi_i\left(q_i, q_j\right) = \frac{\partial \Pi_i}{\partial q_i}.$$

A firm increases (decreases) its quantity if it perceives positive (negative) marginal profit, according to

$$q_i\left(t+1\right) = q_i\left(t\right) + k_i \Phi_i\left(q_i, q_j\right), \tag{3.6}$$

where $k_i > 0$, $i = 1, 2$, is a coefficient that "tunes" the speed of adjustment of firm i's quantity at time $t+1$ with respect to a marginal change in profits when q_i varies at time t.

Therefore, under the above assumptions, the two-dimensional system that characterizes the dynamics of the differentiated Cournot duopoly can be written as follows:

$$T = \begin{cases} q_1' = q_1 + k_1 \left(\frac{\alpha q_1^{\alpha-1} q_2^{\alpha} - c_1 \left(q_1^{\alpha} + q_2^{\alpha}\right)^2}{\left(q_1^{\alpha} + q_2^{\alpha}\right)^2} \right), \\ q_2' = q_2 + k_2 \left(\frac{\alpha q_2^{\alpha-1} q_1^{\alpha} - c_2 \left(q_1^{\alpha} + q_2^{\alpha}\right)^2}{\left(q_1^{\alpha} + q_2^{\alpha}\right)^2} \right), \end{cases} \tag{3.7}$$

where $'$ denotes the unit-time advancement operator, i.e., if q_i is quantity produced at time t then q_i' is production at time $t+1$.

Due to the presence of the denominator, it is obvious that T is defined only at points such that $(q_1, q_2) \neq (0, 0)$; furthermore from an economic point of view we are only interested in the study of positive trajectories, i.e. with points belonging to

the positive quadrant of the plane $\mathbb{R}^2$. Indeed we will consider the feasible region as the set of points in the plane defined by

$$F = \{(q_1, q_2) : q_1 > 0, q_2 > 0\}. \tag{3.8}$$

3.3.1 Local Stability Analysis

In order to study the local stability of the unique Nash equilibrium we localize the eigenvalues of the Jacobian matrix of T evaluated at E^*. Making use of the Jury's conditions, we can state that the Nash equilibrium is locally asymptotically stable if

$$\begin{cases} -A^3k_1k_2 + D_1Bk_2 + D_2Ck_1 > 0, \\ A^4k_1k_2 - 2D_1Bk_2 - 2D_2Ck_1 + D_1D_2 > 0, \end{cases} \tag{3.9}$$

where $A = c_1^\alpha + c_2^\alpha$, $B = [c_2^\alpha(\alpha - 1) - c_1^\alpha(\alpha + 1)]$, $C = [c_2^\alpha(1 + \alpha) + c_1^\alpha(1 - \alpha)]$, $D_1 = \alpha c_1^{\alpha-2}c_2^\alpha$ and $D_2 = \alpha c_2^{\alpha-2}c_1^\alpha$. The two conditions (3.9) define a region in the plane of the speeds of adjustment (k_1, k_2) whose shape is like the shaded area in Fig. 3.2.[3] This region is bounded by the two branches of hyperbola, whose equation is given by the vanishing of the left hand side of

$$-A^3k_1k_2 + D_1Bk_2 + D_2Ck_1 > 0,$$

and the curve represented by the vanishing of the left hand side of

$$A^4k_1k_2 - 2D_1Bk_2 - 2D_2Ck_1 + D_1D_2 > 0.$$

For values of (k_1, k_2) inside the stability region the Nash equilibrium E^* is a stable steady state. The boundaries given by two branches of hyperbola on the left and on the right represent bifurcation curves at which E^* loses its stability through a period doubling (or *flip*) bifurcation. The hyperbola in the central portion represents the bifurcation curve at which the Nash equilibrium is destabilized via NS bifurcation. The lines OI_1 and OI_2 of Fig. 3.2 represent pairs of (k_1, k_2) for which $Tr^2J - 4detJ = 0$ and separate real and complex eigenvalues regions.[4] From the stability conditions we can obtain direct information on the effects of the speed of adjustment, k_1 and k_2, on the local stability of E^*. In particular, an increase of the parameters k_i, with the other parameters fixed, may turn the Nash equilibrium unstable through a flip or a NS bifurcation.

[3] We computed the stability region for $c_1 = 0.1$ and $c_2 = 0.9$ to better visualize the NS bifurcation curve. With different values of marginal costs, the structure of the stability region does not change and only the stable focus region becomes smaller and smaller.

[4] When $c_1 = c_2 = c$, such a condition reduces to $(16c^4\,(k_2 - k_1)^2)/\alpha^2 < 0$ which is never satisfied. Hence no NS bifurcation can occur in the case of symmetric game.

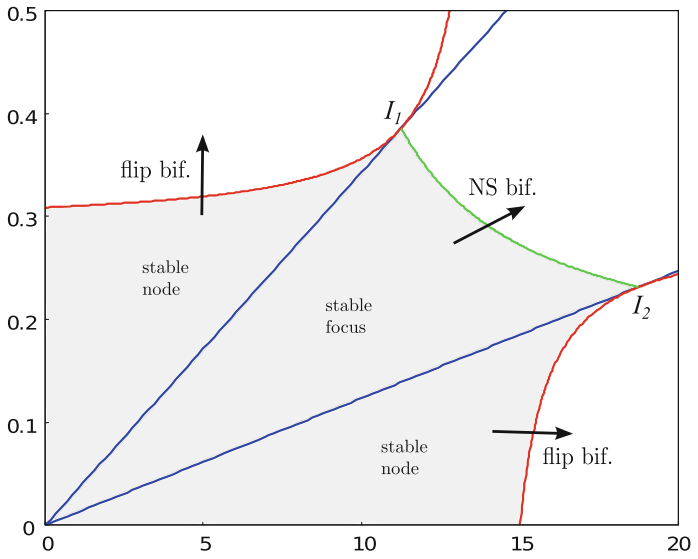

Fig. 3.2 Stability region of the Nash equilibrium. The *shaded gray area* represents the region of local asymptotic stability of the Nash equilibrium in the parameter plane of speeds of adjustment (k_1, k_2). It is noteworthy that if $c_1 = c_2$, the two intersection points I_1 and I_2 coincides

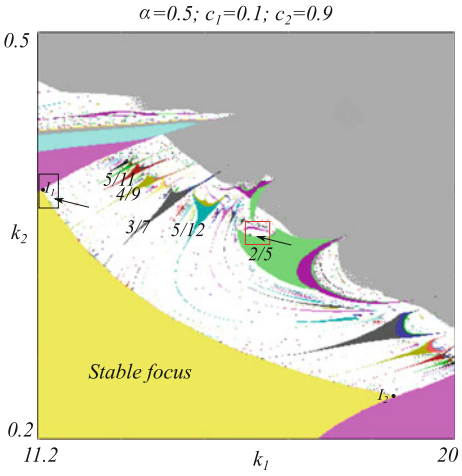

Fig. 3.3 2D bifurcation diagram of the map T in the (k_1, k_2) parameter plane. The different colors are associated with cycles of different period. *White points* correspond to cycles of large period, quasi-periodic trajectories (when close to the NS bifurcation curve) or to complex dynamics. *Gray points* correspond to unfeasible trajectories

Numerical simulations allow us to find out that the NS bifurcation is of supercritical type and it gives rise to an attractive closed invariant curve around the unstable equilibrium, which is a focus. In the 2D bifurcation diagram of Fig. 3.3 the so-called Arnold's tongues issue from the NS bifurcation curve, as we said in Sect. 3.2.

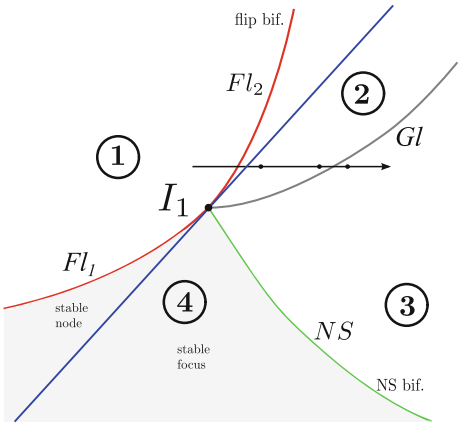

Fig. 3.4 Enlargement of the bifurcation diagram around the co-dimension 2 bifurcation point $R1:2$. The *dots* on the *arrow* correspond to the sequence of Fig. 3.5

3.3.2 Co-dimension 2 Bifurcation

As the 2D bifurcation diagram of Fig. 3.3 shows, many periodicity regions exist, which are organized following the Farey structure. In order to show some dynamic features that take place in this Cournot setting with differentiated goods, we analyze two portions of the 2D bifurcation diagram, highlighted through squares in Fig. 3.3. In particular we first analyze the dynamics around the intersection point I_1 between the NS and the flip bifurcation curves (see Fig. 3.2). In so doing, we study the global bifurcations occurring around the co-dimension 2 bifurcation, the strong resonance $R1:2$ (see [13]), where the eigenvalues are $\lambda_{1,2}=-1$ (an enlargement is reported in Fig. 3.4).

In region 1, the Nash equilibrium E^* is a saddle and coexists with a stable cycle C of period 2 (created at the crossing of the curve Fl_1). Its stable set separates the basins of attraction of the two stable fixed points of the second iterate of the map. Following the path indicated by the arrow in Fig. 3.4, the crossing of the curve $Fl2$ causes a second flip bifurcation of the equilibrium point E^*, that becomes an unstable node, and a saddle cycle $\widetilde{C}$ of period 2 appears. In Fig. 3.5a, the Nash equilibrium E^* is turned into an unstable focus. The attractor of the map is still the 2-cycle C, and the two fixed points of T^2 (second iterate of T) have basins of attraction separated by the stable set of $\widetilde{C}$. The unstable set of $\widetilde{C}$, which is depicted in gray, gives rise to a saddle-node connection: in particular, in Fig. 3.5a, the branch $\alpha_1(\widetilde{C_2})$ converges to C_1 while the branch $\alpha_2(\widetilde{C_2})$ converges to C_2 and the two branches of $\alpha(\widetilde{C_1})$ behave analogously. We also observe that a branch of the unstable set of the saddle 2-cycle issuing from the point $\widetilde{C_2}$, i.e. $\alpha_1(\widetilde{C_2})$, approaches the point $\widetilde{C_1}$ before converging to C_1, signaling that a global bifurcation is likely to occur. In fact, as the parameter k_2 slightly increases, we observe the coexistence of the stable 2-cycle C with an attractive closed invariant curve (see Fig. 3.5b). The appearance of such a curve may be due to a saddle-connection: the unstable set issuing from the point $\widetilde{C_1}$ (previously converging to C_2) reaches the periodic point $\widetilde{C_2}$ (becoming one of its stable branches)

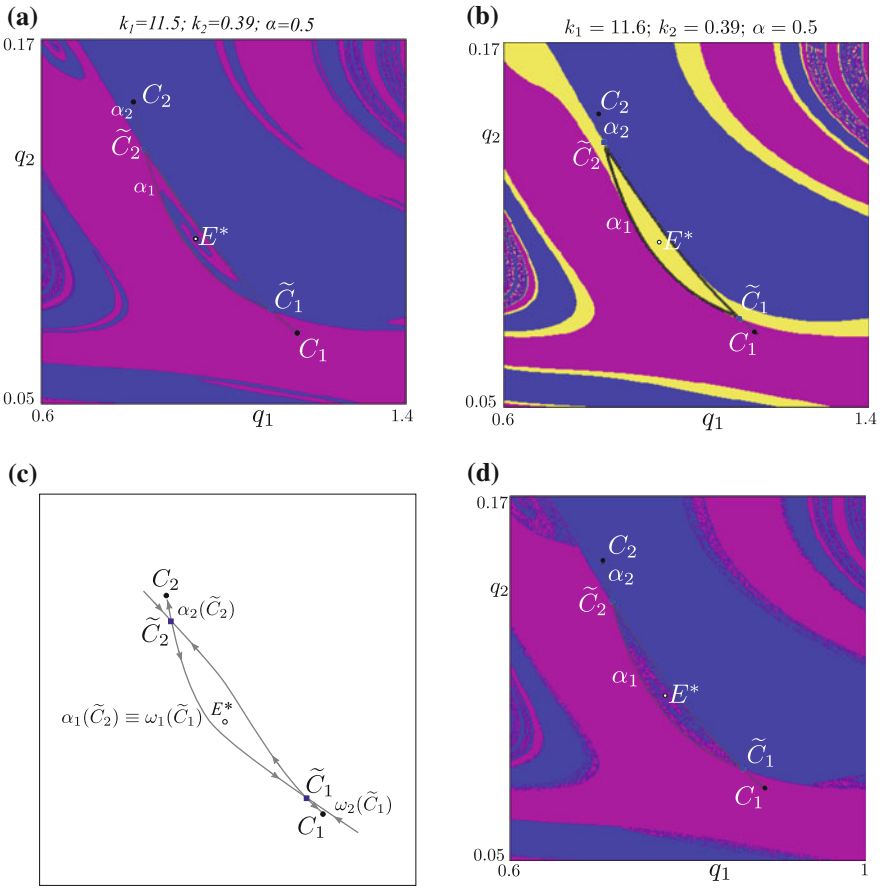

Fig. 3.5 Global bifurcation leading to the appearance of an attracting closed curve. The basins of attraction of the second iterate of the map are represented in order to show the invariant sets of the saddles. **a** Saddle node connection made up by the unstable set of $\widetilde{C}$. **b** An attracting closed curve coexists with the stable 2-cycle C. **c** A qualitative sketch of the saddle connection associated with the appearance of the curve. **d** New fractal portions of the basin of attraction suggesting the possible occurrence of a homoclinic tangle

and, vice versa, the unstable set issuing from the point $\widetilde{C_2}$ (previously converging to C_1) reaches the periodic point $\widetilde{C_1}$ (becoming one of its stable branches) leading to a closed curve (this is shown qualitatively in Fig. 3.5c). As a confirm, one can notice that before the bifurcation the basin of attraction (for the map T^2) of the point C_1 (and similarly for C_2) includes the stable sets of both $\widetilde{C_1}$ and $\widetilde{C_2}$ while, after the bifurcation, for the second iterate of the map the basin of each attracting node is bounded by the stable set of only one saddle fixed point. Moving towards the NS bifurcation curve denoted by NS in Fig. 3.4, the cycles C and $\widetilde{C}$ merge and disappear in a saddle-node bifurcation. The closed invariant curve remains the unique attractor

and becomes smaller and smaller. Finally, at the crossing of the NS curve, a reverse supercritical NS bifurcations occurs and it leaves the Nash equilibrium E^* as the unique attractor.

Before concluding, we observe that the bifurcation mechanism sketched in Fig. 3.5c is simply a schematic representation. Indeed we are dealing with a discrete model and thus it is possible that a homoclinic tangle occurs, that is in a certain parameter range the contact between the stable and unstable set is opened by their quadratic tangency, at which homoclinic orbits appear (and related complex dynamics), followed by transverse intersection and closed by a second quadratic tangency at the opposite side which destroys all the homoclinic orbits. Figure 3.5d seems to suggest this occurrence: the basins of attraction may have a fractal structure close to

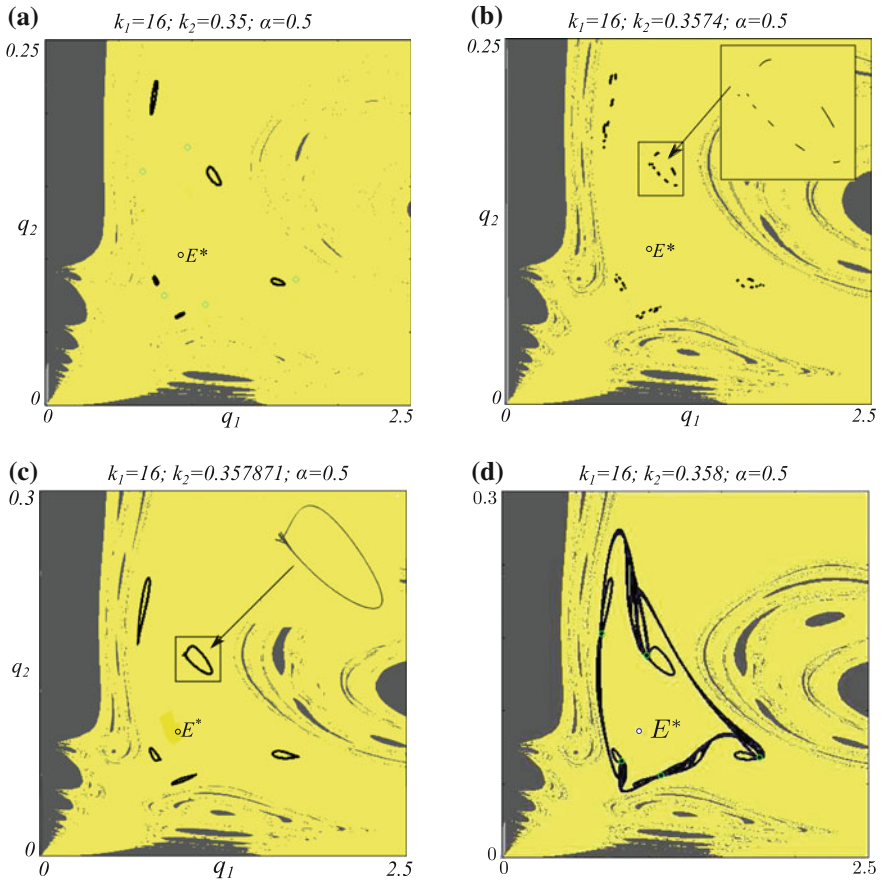

Fig. 3.6 A route to chaotic dynamics. The parameter values are chosen close to the periodicity region of the 5-cycle. The *green circles* denote the period 5 saddle cycle. **a** 5 cyclical attracting closed curves due to NS bifurcation. **b** 40-piece chaotic attractor due to a period doubling sequence. **c** Cyclical attractor made up of 5 weakly chaotic rings. **d** A unique annular chaotic attractor

the saddles and to their preimages. These particular basins' regions are similar to the ones that can be already observed in Fig. 3.5a, but they appear only in the portions of the phase-space that will become the basin of attraction of the closed curve (compare Fig. 3.5b, d).

3.3.3 A Route to Chaos

We now analyze the dynamics of the model when the parameters are chosen close to the tongue associated with a 2/5 attracting cycle, as highlighted through the red square in Fig. 3.3. This allows us to show that besides the period doubling sequence, the model exhibits also a different route to chaotic dynamics. In such a periodicity region, a stable 5-cycle exists as well as a saddle cycle of the same period. Keeping the value of k_1 fixed at 16.2, we increase the value of k_2 and at the crossing of the boundary of the periodicity region indicated by an arrow in Fig. 3.3 we observe the occurrence of a supercritical NS bifurcation of the period 5 stable cycle. Then, immediately after such a crossing, 5 cyclical attracting closed curves exist in the phase space, as shown in Fig. 3.6a. If the parameter k_2 further increases, different phase locking situations take place and one of them (associated with 5 saddle-node connections of two cycles of period 8) undergoes a period doubling sequence that gives rise to the 40 pieces chaotic attractor shown in Fig. 3.6b with its enlargement. Then a homoclinic bifurcation of the 5 saddle cycle of period 8 causes the appearance of the cyclical attractor shown in Fig. 3.6c; the enlargement of one piece of the attractor allows us to appreciate that each closed curve exhibits loops and self-intersections. This means that the cyclical attractor is made up of 5 weakly chaotic rings (see [15]) that merge in a unique annular chaotic attractor when k_2 is further increased and a homoclinic bifurcation of the saddle cycle of period 5 occurs, as shown in

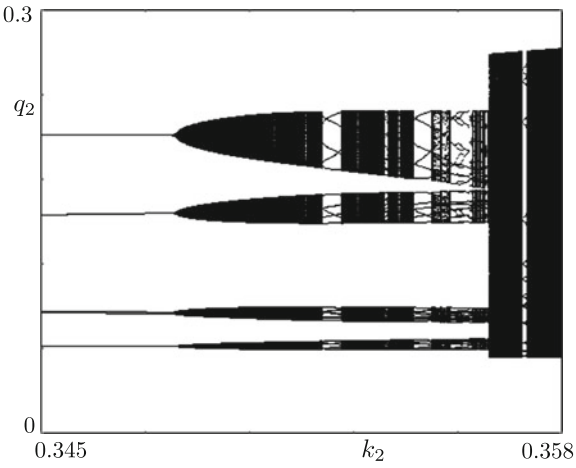

Fig. 3.7 1D bifurcation diagram with respect to k_2. As the parameter k_2 increases, different bifurcations occur which finally give rise to a unique annular chaotic attractor

Fig. 3.6d. The bifurcation diagram in Fig. 3.7 shows the latter bifurcation path and summarizes the sequence of bifurcations leading to the appearance of the annular chaotic attractor.

3.4 An Advertising Cournot Model: Subcritical NS Bifurcation

The second example we propose is a particular case of a Cournot triopoly where firms face markets in several countries. The basic features of this model are the unimodal reaction functions, obtained with the assumptions of isoelastic demand function, constant marginal costs, and an adaptive adjustment of the strategic variable.

The model is based on the following assumptions:

(i) there are three firms on the market that produce perfect substitute goods; they produce the commodity quantities q_i and distribute their products in several countries making use of x_i quantities of advertising ($i = 1, 2, 3$);
(ii) x_i is the strategic variable, to focus on the marketing issue; we disregard the production costs and c_i is the cost per unit of advertisement;
(iii) two of the competing firms produce the same commodity, equally behave in production and marketing policy, (i.e., $q_1 = q_3$ and $x_1 = x_3$) and have equal advertisement cost.

Further, we assume that the exponents of the Cobb-Douglas utility functions depend on advertising expenditures by the competitors, more precisely that the exponents are the shares of each firm in total advertising expenditures of all competitors. Then the consumers' demand is:

$$U = q_1^{\frac{x_1}{x_1+X_1}} q_2^{\frac{x_2}{x_2+X_2}} q_3^{\frac{x_3}{x_3+X_3}}, \tag{3.10}$$

where X_i, $i = 1, 2, 3$, denotes the advertising expenditure of competitors of firm i.

Therefore, utility maximizing consumer disposing of one monetary unit in the budget spends

$$p_i q_i = \frac{x_i}{x_i + X_i} \tag{3.11}$$

on each commodity. From the producer point of view, (3.11) represents the revenue of the firm. In this way, we can consider both the situation when the producers set prices or quantities, as this will not affect the results.

Finally, the optimization of profit of producer i leads to the reaction functions depending on the expected productions of competitors ($X_i^{(e)}$):

$$r_i(X_i^{(e)}) = \sqrt{\frac{X_i^{(e)}}{c_i}} - X_i^{(e)}. \tag{3.12}$$

From the economic point of view (3.12) only makes sense as long as $0 \leq X_i^{(e)} \leq 1/c_i$, otherwise reaction and profit become negative and the producer can decide either to withdraw or to modify his strategy.

To close the model, we assume that competitors move making use of the "adaptive expectation" mechanism. They give a weight $\theta \in [0, 1]$ to the best calculated reply for their competitors (3.12) and $(1 - \theta)$ to their own previous move x_i. Thus any competitor moves according

$$x_i' = \begin{cases} \theta\left(\sqrt{\frac{X_i}{c_i}} - X_i\right) + (1-\theta)\, x_i, & 0 \leq X_i \leq \frac{1}{c_i}, \\ (1-\theta)\, x_i, & X_i > \frac{1}{c_i}, \end{cases} \tag{3.13}$$

with $i = 1, 2, 3$.

Now, considering assumption (iii) the model (3.13) becomes a 2D map with $X_1 = x_1 + x_2$, $X_2 = 2x_1$. Then the object of our study is the 2D nonlinear map:

$$T : \begin{cases} x' = T_1(x, y), \\ y' = T_2(x, y), \end{cases} \tag{3.14}$$

where

$$T_1(x, y) = \begin{cases} \theta\left(\sqrt{\frac{x+y}{c_1}} - (x + y)\right) + (1-\theta)x, & 0 \leq x + y \leq \frac{1}{c_1}, \\ (1-\theta)x, & x + y > \frac{1}{c_1}, \end{cases} \tag{3.15}$$

and

$$T_2(x, y) = \begin{cases} \theta\left(\sqrt{\frac{2x}{c2}} - 2x\right) + (1-\theta)y, & 0 \leq x \leq \frac{1}{2c_2}, \\ (1-\theta)y, & x > \frac{1}{2c_2}. \end{cases} \tag{3.16}$$

For a sake of simplicity in (3.14) we have denoted with x and y the phase variables x_1 and x_2.

To have meaningful trajectories from the economic point of view, we restrict the analysis of T to the positive orthant of R_2 (feasible region).

The map T in (3.14) depends on three parameters, the two marginal costs, $c_1 > 0$ and $c_2 > 0$, and the "adaptive" coefficient $\theta \in [0; 1]$. However a simple change of coordinates[5] allows us to show that only two parameters, $(c_2/c_1; \theta)$, are essential to study the dynamics of T. Then in the following, without loss of generality, we shall consider the map T with $c_1 = 1$ and the parameter c_2 has to be interpreted as the ratio of the marginal costs.

[5]The coordinate change is $\Psi(x, y) = (c_1 x, c_1 y)$.

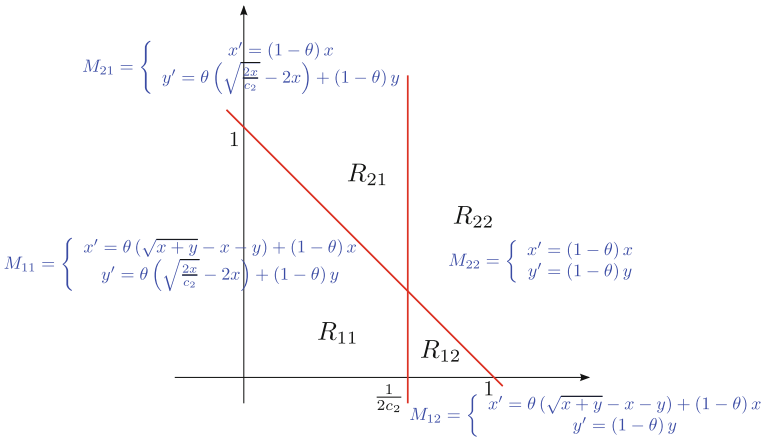

Fig. 3.8 The PW smooth map T. The different branches of the map T and related definition regions

The map T is a continuous piecewise map, then there exist four regions in which T assume a different definition. They are

$$R_{11} = \left\{(x_1, x_2) : 0 \le x_1 \le \frac{1}{2c_2}, 0 \le x_1 + x_2 \le 1\right\}, \tag{3.17}$$

$$R_{12} = \left\{(x_1, x_2) : x_1 > \frac{1}{2c_2}, 0 \le x_1 + x_2 \le 1\right\}, \tag{3.18}$$

$$R_{21} = \left\{(x_1, x_2) : 0 \le x_1 \le \frac{1}{2c_2}, x_1 + x_2 > 1\right\}, \tag{3.19}$$

$$R_{22} = \left\{(x_1, x_2) : x_1 > \frac{1}{2c_2}, x_1 + x_2 > 1\right\} \tag{3.20}$$

and are illustrated in Fig. 3.8.

3.4.1 *Local Stability Analysis*

To look at the fixed points of the map M in (3.13) we consider separately the four regions R_{ij} $(i, j = 1, 2)$ defined in (3.20). We shall denote with M_{ij} the map defined in R_{ij}.

The maps M_{22} and M_{21} admit a unique fixed point $O = (0, 0) \in R_{11}$, then they have a "virtual" steady state; moreover the eigenvalues of the Jacobian matrix are $\lambda_1 = \lambda_2 = 1 - \theta$. This means that any trajectory either in R_{22} or R_{21} leaves the regions in a finite number of steps.

In region R_{12}, besides the origin O, the map M_{12} admits the fixed point $P^* = (1/4, 0)$, always with eigenvalues $\lambda_1 = \lambda_2 = 1 - \theta$. Then when $c_2 > 2$, P^* is a stable equilibrium of M and when $c_2 = 2$ it has a border collision, entering R_{11}. This means that when $c_2 < 2$ the trajectories in R_{12} enter R_{11} in a finite number of steps and, from an economic point of view, are unfeasible since $y < 0$.

Finally, we consider the region R_{11}. The not trivial equilibrium of M_{11} is the Cournot equilibrium point (intersection of the two reaction curves (3.12)) given by $E^* = \left(2c_2/(2+c_2)^2, 2\,(2-c_2)/(2+c_2)^2\right)$. The fixed point E^* is feasible only if $c_2 \leq 2$ and, when feasible, belongs to R_{11}, since the constraint $x_1 + x_2 < 1$ is always satisfied by E^*. While, when $c_2 = 2$, E^* belongs to the constraint $x_1 = 1/2c_2$ and to $x_2 = 0$, and if c_2 increases the Cournot equilibrium enters the region R_{12} and becomes unfeasible.

The analysis just performed allows us to conclude that the map M admits a unique not trivial equilibrium:

1. The Cournot equilibrium E^* if $c_2 < 2$;
2. P^* if $c_2 > 2$, which is always stable.

When $c_2 = 2$ the two fixed points merge and belong to the border line separating regions R_{11} and R_{12}.

Henceforth, we restrict our analysis to the case $c_2 < 2$ to only consider the dynamic behaviors associated with the Cournot equilibrium point. The localization of the eigenvalues of the Jacobian matrix $J(E^*)$ of T evaluated at E^* allows us to state the following

Proposition 3.1 *Let* $(\theta, c_2) \in \Omega = [0, 1] \times (0, 2)$. *The fixed point*

$$E^* = \left(\frac{2c_2}{(c_2+2)^2}, \frac{2(2-c_2)}{(c_2+2)^2}\right)$$

is locally stable if

$$\theta < \theta_{ns} := \frac{2c_2(10-c_2)}{(c_2+2)^2}.$$

Proof See [3]. □

Moreover, it is possible to obtain that the eigenvalues of $J(E^*)$ are complex conjugated in $\widetilde{\Omega} = \left\{(\theta, c_2) : 0 < \theta < 1 \wedge 0 < c_2 < 13 - 3\sqrt{17}\right\}$. Following [11] (Theorem 3.5.2) it is possible to prove the following

Proposition 3.2 *If*

1. $(\theta, c_2) \in \widetilde{\Omega}$ *with* $c_2 \notin \left\{10 - 4\sqrt{6}, \bar{c}_2\right\}$, *where*

$$\bar{c}_2 = \frac{16}{3} + \frac{16\sqrt{7}}{3}\cos\frac{\arctan(\psi) + 2\pi}{3} \quad \textit{with} \quad \psi = \frac{27\sqrt{47}}{563}$$

2. *and* $P_6(c_2) < 0$, *where* $P_6(c_2) = 5c_2^6 + 120c_2^5 - 1372c_2^4 + 4224c_2^3 - 4752c_2^2 + 2176c_2 - 320$,

then at

$$\theta = \theta_{ns} = \frac{2c_2(10 - c_2)}{(c_2 + 2)^2} \tag{3.21}$$

the fixed point E^* *undergoes a subcritical Neimark-Sacker bifurcation.*

Proof Proposition 3.1 states that if $\theta < \theta_{ns}$ the fixed point is a stable focus (the two eigenvalues forming a complex conjugated pair) and it becomes an unstable focus when θ exceeds θ_{ns}. Then the complex eigenvalues of $J(E^*)$ have modulus one when (3.21) holds. Moreover, it is possible to verify that if $c_2 \notin \left\{10 - 4\sqrt{6},\ \bar{c}_2\right\}$ then $\lambda^n \neq 1,\ n = 1, 2, 3, 4$. Thus strong resonance cases are excluded. Finally, computing the coefficients d and a of Theorem 3.5.2 in [11, p. 162], we obtain $d = (10 - c_2)/8 > 0$ and $a > 0$ if $P_6(c_2) < 0$.[6] This proves that a subcritical NS bifurcation takes place at $\theta = \theta_{ns}$. □

From Proposition 3.2, we also obtain that the parameter value $(\theta_{ns}(\bar{c}_2),\ \bar{c}_2) \in \widetilde{\Omega}$ corresponds to a $1:3$ resonant case and $\left(\theta_{ns}\left(10 - 4\sqrt{6}\right),\ 10 - 4\sqrt{6}\right) \in \widetilde{\Omega}$ to a $1:4$ resonant case. This means that at these parameter values the closed invariant curve might appear in a very peculiar way, or there might be several invariant curves bifurcating from the fixed point.

Numerical investigation allows us to find out that condition (b) holds if $c_2 < \hat{c}_{ch}$, with $\hat{c}_{ch} \approx 0.2769$. The parameter values $\hat{C} = \left(\theta_{ns}\left(\hat{c}_{ch}\right),\ \hat{c}_{ch}\right)$ correspond to a Chenciner point. This means that in the parameter space $\widetilde{\Omega}$ a (global) bifurcation curve γ originates from $\hat{C}$ and enters the region in which E^* is stable. The crossing of such a curve causes the appearance of two invariant closed curves, one attracting and one repelling, the latter being involved in the occurring NS bifurcation. The study of the global bifurcations occurring along the curve γ is our present aim.

As in Sect. 3.3, we start our analysis looking at a 2D-bifurcation diagram, shown in Fig. 3.9. In such a figure we can observe that the Arnold's tongues have a particular "sausage" shape, typical of PW maps. Indeed, the boundaries of these periodicity regions are given by BCB's and their "narrowed" portions correspond to the crossing of one periodic point through a boundary of a region R_{ij}, associated with a border collision which preserves the existing attractor.

Comparing Fig. 3.9 with Fig. 3.3 a second peculiarity emerges: in the former figure the Arnold tongues appear when the fixed point is still stable and intersect the θ_{ns} bifurcation curve. As we said in Sect. 3.2, this is due to the Neimark-Sacker bifurcation (NS) of subcritical type, as we proved, and indicates that a pair of cycles must appear in the phase-space and coexists with the stable fixed point E^* (see also [4]).

[6] For major details see [3].

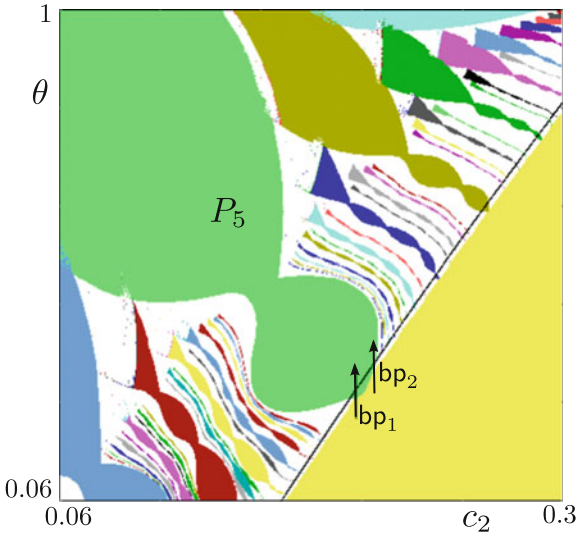

Fig. 3.9 2D bifurcation diagram. The Arnold's tongues of the PW map T have the "sausage" structure

To investigate the bifurcation mechanisms leading to the appearance of the invariant closed curves, at the crossing of the curve γ, we follow the bifurcation paths indicated with an arrow in Fig. 3.9, since simple cycles of period 5 will be involved.

3.4.2 *Appearance of Curves Due to Homoclinic Bifurcation*

We start considering the bifurcation path bp_1 in which $c_2 = 0.1306$. At the crossing of the boundary of the region P_5 a pair of cycles of period 5 appears, a saddle cycle S and an attracting one C. As shown in Fig. 3.10a, at their appearance the two cycles are very close to each other and close to the line separating region R_{11} from region R_{21}. This suggests that the appearance of the cycles may be due to a "saddle-node" BCB.

The basins of attraction of the two coexisting attractors are separated by the stable set $W^s(S) = \omega_1 \cup \omega_2$ of the saddle cycle S and no invariant curve exists immediately after the occurrence of the BCB. Indeed, the branch α_1 of the unstable set $W^u(S) = \alpha_1 \cup \alpha_2$ of S goes to E^* while α_2 converges to the cycle C. Increasing the parameter θ the stable branch ω_1 approaches the unstable branch α_1, as we can observe in Fig. 3.10b. More precisely, if we consider separately the periodic points S_s, with $s = 1, \ldots, 5$, of the saddle cycle S and $\omega_i = \bigcup_{s=1}^{5} \omega_{i,s}$, $\alpha_i = \bigcup_{s=1}^{5} \alpha_{i,s}$ with $i = 1, 2$, we have that $\omega_{1,s}$ is closer and closer to $\alpha_{1,s+1}$ ($s = 1, \ldots, 5$ and $\alpha_{1,6}$=$\alpha_{1,1}$). This means that a heteroclinic connection (or "heteroclinic loop") between the periodic points of the saddle cycle may be near to occur. This seems exactly the same situation described in Sect. 3.2. Indeed, if we slightly increase θ as in Fig. 3.10c (passing from 0.5635 to 0.5636), we observe that two invariant closed curves appear,

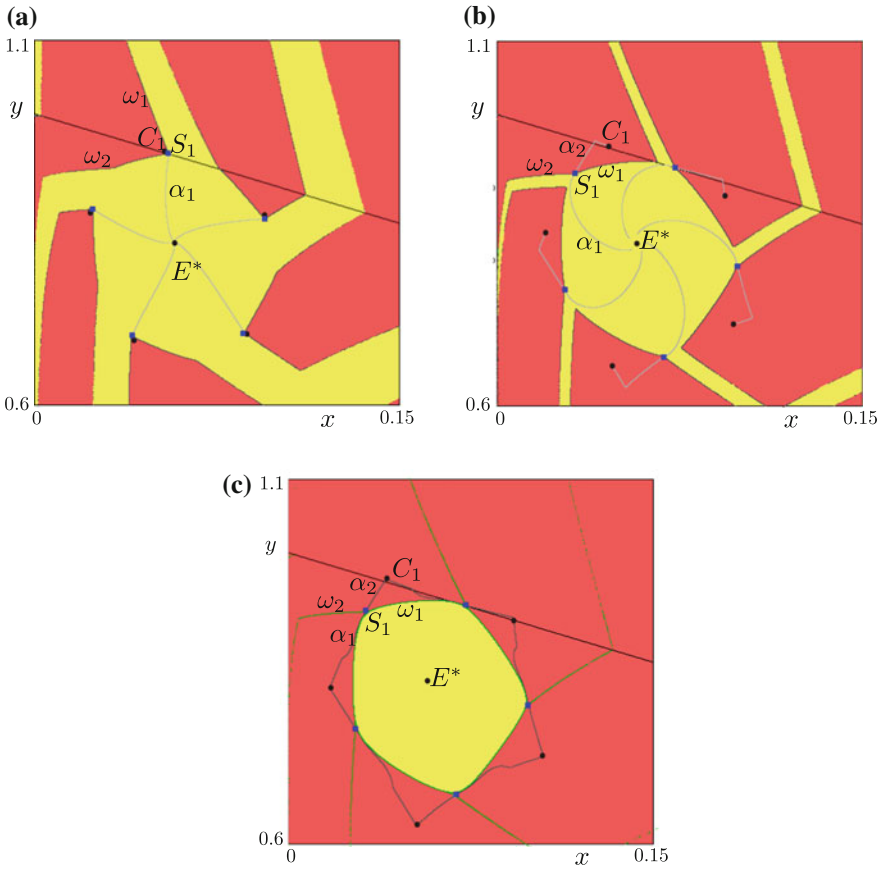

Fig. 3.10 Appearance of two invariant closed curves. Along the bifurcation path bp_1 a homoclinic bifurcation occurs. **a** $\theta = 0.562683$. The cycle of period 5 appears via BCB. **b** $\theta = 0.5635$. No closed curves exist. **c** $\theta = 0.5636$. Two invariant closed curves appear

one stable made up by the unstable set $W^u(S)$ which connects the periodic points of C and one unstable which bounds the basin of attraction of E^*. This means that the curve γ associated with the Chenciner point has been crossed.

To confirm that a homoclinic bifurcation occurs, we propose two further figures. Figure 3.11 represents the phase-plane immediately before the bifurcation: no invariant closed curve exists but we can observe that both stable and unstable set are wandering and quite tangent (see the enlargements in Fig. 3.11b). Then a homoclinic tangle start to develop and transverse crossing between the two invariant sets arise in a small parameter range. At the closure of the homoclinic tangle, the branches α_1 and ω_1 are again tangent, but at the opposite side, as Fig. 3.12 shows, and two invariant curves appear. To sum up, we remark that along the bifurcation curve bp_1

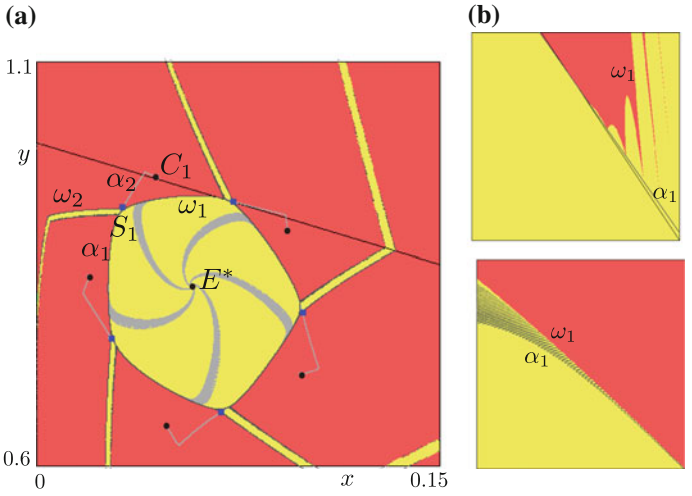

Fig. 3.11 Homoclinic tangle. The first tangential contact between the stable and unstable sets of the saddle cycle S. **a** $\theta = 0.56357725$. The branches α_1 and ω_1 exhibit many oscillation and are quite tangent. **b** Enlargement of stable and unstable sets

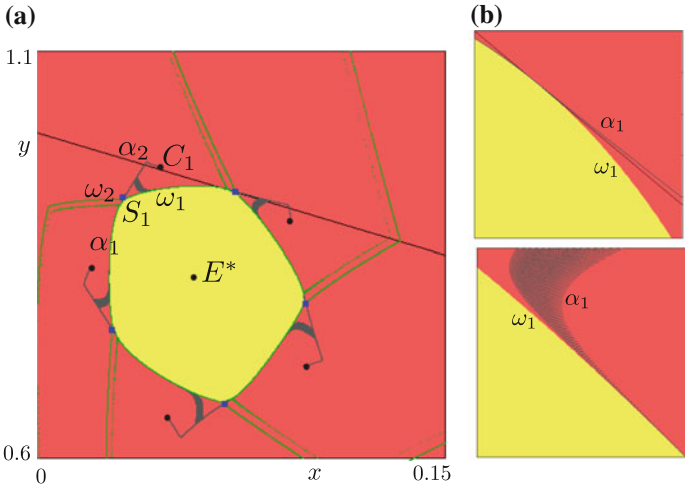

Fig. 3.12 Homoclinic tangle. The second tangential contact between the stable and unstable sets of the saddle cycle S. **a** $\theta = 0.56357729$. The branches α_1 and ω_1 have exchanged their mutual position and two invariant closed curves exist, very close each other. **b** Enlargement of the stable and unstable sets

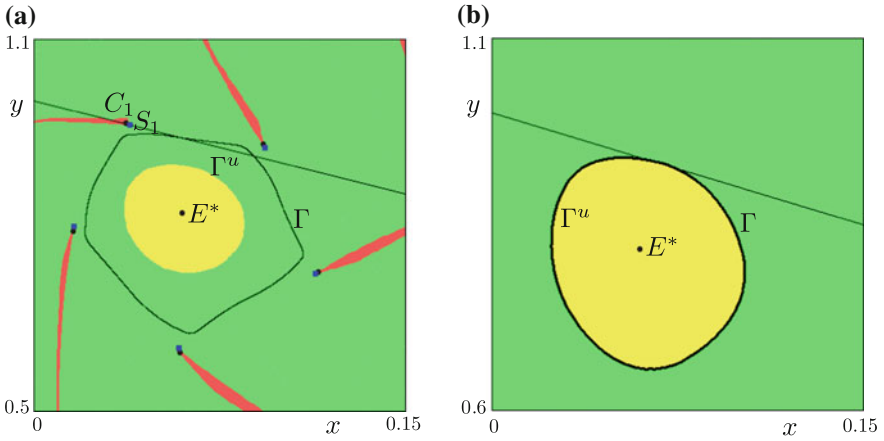

Fig. 3.13 Appearance of two invariant closed curves. Along the bifurcation path bp_2 a BCB causes the appearance of two invariant closed curves. **a** $\theta = 0.5825$. Three coexisting attractors. **b** $\theta = 0.5795$. Appearance of the closed invariant curves

the crossing of the curve γ (that is, the appearance of two invariant closed curves) occurs when a homoclinic bifurcation takes place.

3.4.3 Appearance of Curves Due to BCB

A different bifurcation mechanism arises along the bifurcation path bp_2 where $c_2 = 0.135$. Indeed, as shown in Fig. 3.13a, when the two cycles of period 5 appear, at $\theta = 0.5825$, the two curves Γ and Γ^u already exist. The bifurcation leading to the appearance of C and S seems again a "saddle-node" BCB and after its occurrence we have the coexistence of three attractors: the period 5 cycle C whose basin of attraction is bounded by the stable set of the saddle cycle S, the attracting closed curve Γ and the Cournot equilibrium E^*. A repelling closed curve Γ^u separates the basins of attraction of these two last attractors. This means that the bifurcation curve γ do not intersect the periodicity region P_5 along bp_2.

To investigate when the two invariant closed curves appear we decrease the parameter θ and we find that at $\theta = 0.5795$ the two curves are quite indistinguishable (see Fig. 3.13b) and the attracting one appears quite tangent to the border separating region R_{11} from region R_{21}. This suggests that a BCB can be the cause of the appearance of Γ and Γ^u.

To show that this is really the case we consider the map M_{11}, since in the parameter plane under scrutiny the Cournot equilibrium point is a fixed point of it.

The global analysis of the map M_{11} allows us to show that when being stable the fixed point E^* has a basin of attraction which contains all the feasible trajectories. If we consider $\theta = 0.579$, very closed to the value previously identified, the basin of attraction of E^* is bounded by a repelling closed curve Γ^u (see Fig. 3.14a) an its very small portion (denoted with a white arrow) belongs to region R_{21}. This implies

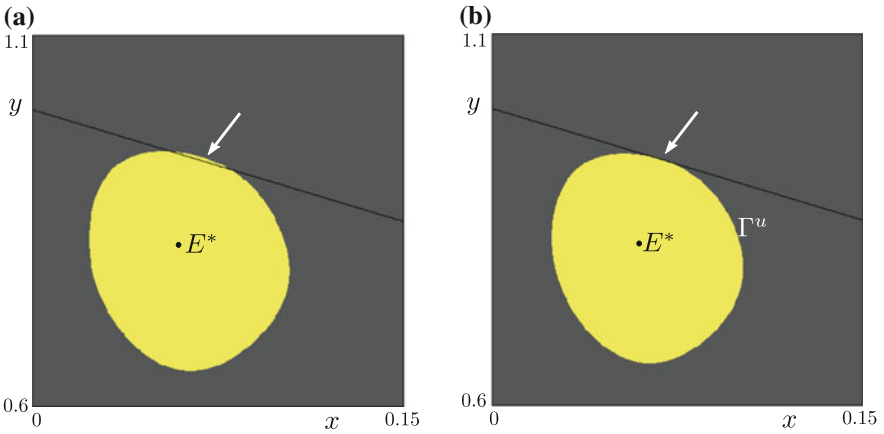

Fig. 3.14 The map M_{11}. A repelling closed curve bounds the set of feasible trajectories. **a** $\theta = 0.579$. The basin of attraction of E^*. **b** $\theta = 0.5795$. Border collision of an invariant closed curve

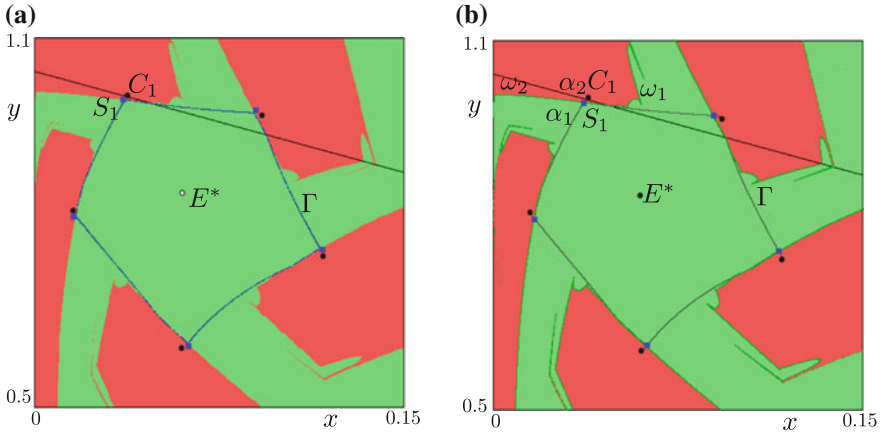

Fig. 3.15 After the occurrence of the Neimark-Sacker bifurcation. At $\theta = 0.5895$ only two attractors survive. Their basins of attraction are separated by the stable set of S. **a** The attracting closed curve coexists with the period 5 cycle C. **b** The unstable and stable sets of the saddle cycle S

that when we consider the map M such portion will be iterated with the map M_{21} and consequently all the unfeasible points disappear from the phase space of map M.

Coming back to the map M_{11}, when θ increases this portion becomes smaller and smaller and finally, at $\theta = 0.5795$ it disappears (see Fig. 3.14b). When the portion disappears, the boundary of the set of feasible trajectories of M_{11} becomes tangent to the border line $x_1 + x_2 = 1$. This means that Γ^u is an invariant set of M_{11} belonging to the region R_{11} and then is an invariant set also of the map M. Moreover the points of region R_{21}, all unfeasible for M_{11}, have a different behavior when iterated by M, that is a further attractor has to be appear. This is exactly what we have observed in Fig. 3.13b. Then we can conclude that along the bifurcation path bp_2 a different

bifurcation mechanism occurs when the curve γ is crossed, since a BCB has caused the appearance of two invariant closed curves.

Nevertheless, a homoclinic bifurcation occurs even along bp_2. Increasing the parameter θ, firstly we observe the occurrence of the subcritical NS bifurcation. Then E^* becomes an unstable focus and only two attractors survive, the period 5 cycle C and the closed curve Γ, as in Fig. 3.15a. The basins of attraction are still separated by the stable set $W^s(S)$ of the saddle S. But, as we can observe in Fig. 3.15b, the branch ω_1 of $W^s(S)$ exhibits some fluctuations before converging to S and it is very close to the branch α_1 of $W^u(S)$. As we have seen above, this is exactly the prelude of the occurrence of a homoclinic bifurcation. Indeed, if we slightly increase the parameter θ the branches ω_1 and α_1 change their reciprocal position and, in particular, ω_1 now come from E^* (see Fig. 3.16). Then a homoclinic bifurcation has occurred and it has

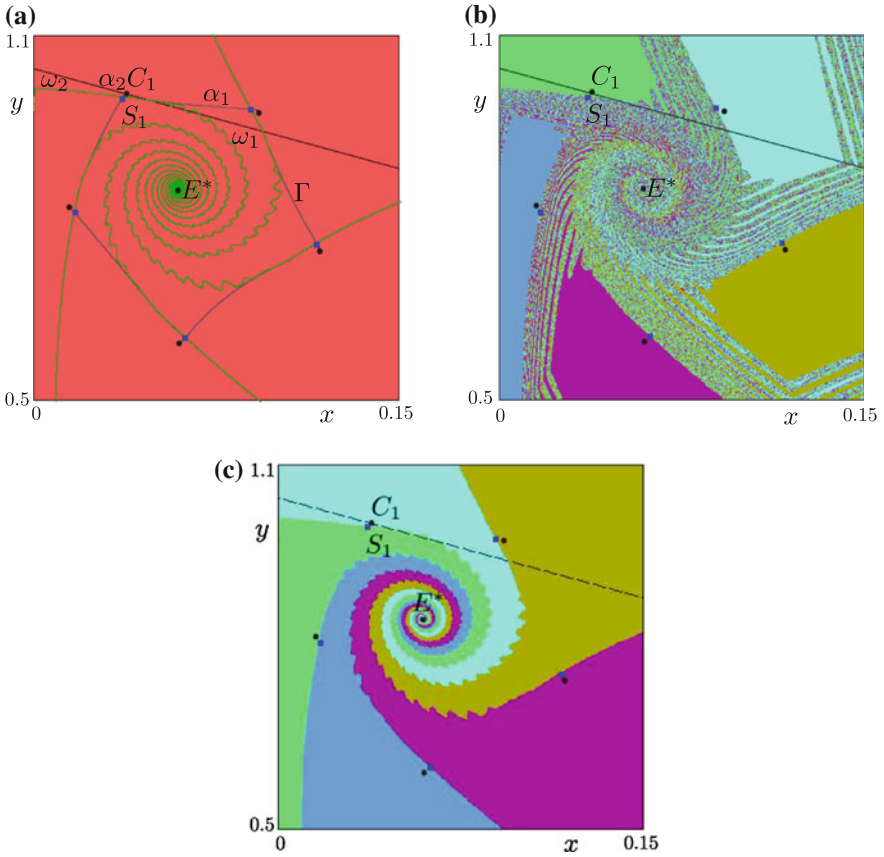

Fig. 3.16 The 5-cycle C is the unique attractor. A homoclinic bifurcation has caused the disappearance of the attracting closed curve Γ. **a** $\theta = 58995$. The closed curve Γ has disappeared. **b** $\theta = 0.5898$. The basins of attraction of the 5 fixed points of the map M^5 are strongly mixed. **c** $\theta = 58995$. The complex structure of the basins of attraction does not exist

caused the disappearance of the attracting closed curve Γ. To illustrate the effect of the occurring homoclinic bifurcation we consider the 5th iterate of the map M. The map M^5 undergoes five simultaneous homoclinic bifurcations, as proved by the fractal structure of the basins of attraction of its stable fixed points C_s, $s = 1, \ldots, 5$, due to the presence of a chaotic repellor (see Fig. 3.16b). This particular structure of the basins immediately disappears when the second tangential contact between ω_1 and α_1 occurs, as shown in Fig. 3.16.

3.5 Conclusions

Several studies have been devoted to the NS bifurcations of fixed points in two-dimensional maps describing oligopoly models. In this paper we focused on the problem related to the mechanism giving rise to the appearance/disappearance of invariant closed curves, attracting and/or repelling. Considering duopoly models in which the Cournot equilibrium is destabilized through a supercritical or a subcritical NS bifurcation, we have shown that such bifurcations may give rise to different dynamic behavior, depending on the type of map we are dealing with. The first model deals with a smooth map and, through global analysis, we have shown different multistability situations and the occurrence of global bifurcations associated with the appearance of invariant closed curves and chaotic dynamics. The second model, instead, is described by a PW map where the Cournot equilibrium point coexists with an attracting closed curve and it is destabilized through a subcritical NS bifurcation. We have shown that the mechanism related to the appearance/disappearance of invariant closed curves is related to homoclinic and border collision bifurcations.

A final remark is about the economic implication of the global bifurcations: given the attention paid in the economic literature to the onset of endogenous and long-run fluctuations, the bifurcation scenario we have detected may find important applications. Indeed, it implies multistability situations and may deserve to explain phenomena like hysteresis loops and catastrophic transitions.

Acknowledgments Authors thank Ahmad Naimzada and Tönu Puu for their many valuable suggestions and remarks about the two oligopoly settings.

References

1. Agliari, A., Bischi, G.I., Dieci, R., Gardini, L.: Global bifurcations of closed invariant curves in two-dimensional maps: a computer assisted study. Int. J. Bifurcat. Chaos **15**(4), 1285–1328 (2005)
2. Agliari, A., Naimzada, A., Pecora, N.: Nonlinear dynamics of a Cournot duopoly game with differentiated products. Appl. Math. Comput. (2016)
3. Agliari, A., Puu, T., Szuz, A.: The dynamics of a particular triopoly game when two competitors become identical. Mimeo

4. Agliari, A., Gardini, L., Puu, T.: Global bifurcation in duopoly when the Cournot point is destabilized via a subcritical neimark bifurcation. Int. Game Theory Rev. **8**(1), 1–20 (2006)
5. Ahmed, E., Elsadany, A.A., Puu, T.: On bertrand duopoly game with differentiated goods. Appl. Math. Comput. **251**, 169–179 (2015)
6. Boyland, P.L.: Bifurcations of circle maps: Arnol'd tongues, bistability and rotation intervals. Commun. Math. Phys. **106**, 353–381 (1986)
7. Chenciner, A.: Bifurcations de points fixes elliptiques : III—orbites pèriodiques de "petites" pèeriodes et èlimination rèsonnante des couples de courbes invariantes. Publications de l'I.H.E.S. **66**(1), 5–91 (1987)
8. Gardini, L., Puu, T., Sushko, I.: The hicksian floor-roof model for two regions linked by interregional trade. Chaos Solitons Fractals **18**, 593–612 (2003)
9. Gardini, L., Sushko, I.: Doubling bifurcation of a closed invariant curve in 3d maps. ESAIM: Proc. **36**, 180–188 (2012)
10. Guckenheimer, J., Holmes, P.: Nonlinear Oscillations, Dynamical Systems, and Bifurcations of Vector Fields, vol. 42. Springer (1983)
11. Guckenheimer, J., Holmes, P.: Nonlinear Oscillations and Dynamical Systems and and Bifurcations of Vector Fields. Springer, New York (1985)
12. Gumovsky, I., Mira, C.: Dynamique Chaotique: Transformations Ponctuelles. Transition Ordre - Désordre. Collection Nabla. Cépaduès Édition, Toulouse (1980)
13. Kuznetsov, Y.A.: Elements of Applied Bifurcation Theory. Springer (2013)
14. Martin, S.: Advanced Industrial Economics, 2 edn. Wiley-Blackwell (2002)
15. Mira, C., Gardini, L., Barugola, A., Cathala, J.C.: Chaotic Dynamics in Two-dimensional Noninvertible Maps. Nonlinear Science. World Scientific, Singapore (1996)
16. Nusse, H., Ott, E., Yorke, J.: Border-collision bifurcations: an explanation for observed bifurcation phenomena. Phys. Rev. E **49**, 1073–1076 (1994)
17. Nusse, H.E., Yorke, J.A.: Border-collision bifurcations including 'period two to period three' for piecewise smooth systems. Phys. D **57**, 39–57 (1992)
18. Nusse, H.E., Yorke, J.A.: Border-collision bifurcations for piecewise smooth one-dimensional maps. Int. J. Bifurcat. Chaos **5**(1), 189–207 (1995)